Real-Time Imaging **1**, 19–31 (1995)

Iterative Restoration Algorithm for Real-Time Processing of Broadband Synthetic Aperture Sonar Data

Broadband synthetic aperture sonar (SAS) is a high resolution underwater imaging technique, which uses a digital matched filter for pulse compression followed by aperture synthesis, also referred to as azimuthal matched filtering, to improve resolution. Thus, the processing scheme is equivalent to a two-dimensional matched filter operation, in which the point spread function (PSF) for the particular SAS-geometry considered is correlated with the observation. It can be shown that this processing scheme is suboptimal, because it causes a blurring of the processed image. Therefore, the purpose of this paper is to develop a computationally efficient iterative algorithm for reconstruction, which compares effectively to the matched filter in the processing time, but shows significant improvement in image detail. The proposed iterative restoration algorithm is derived by modifying the optimal gradient method through an adaptive relaxation technique. The adaptivity is introduced to incorporate properties of the true restoration error. This makes the successive approximations approach the exact solution much faster, enabling a visually good convergence within a few iterates. Asymptotic convergence of the proposed iterative algorithm is established. For the experimental results which are shown, the new algorithm performs better on accuracy and compares well on computation time. Application to underwater object imaging using simulated data shows clear improvements compared to a matched filter processing technique.

E. Ochieng-Ogolla,* S. Fischer,* A. Wasiljeff* and Ph. de Heering†

**University of Bremen, Dept. of Physics and Electrical Engineering, P.O. Box 330440, D-28334 Bremen, Germany. E.mail: ochieng.@physik.uni-bremen.de*

†European Patent Office, Patentlaan, 2, Rijswijk, The Netherlands

Introduction

There are a number of applications where underwater imaging systems are required to generate images with high enough fidelity necessary for accurate image interpretation. But, the physical nature of the ocean environment places various limitations upon the ability to image underwater objects using synthetic aperture techniques. Factors such as low sound speed, attenuation, platform stability, and reverberation (1,2) place constraints on imaging parameters such as resolution and area coverage rate. Undersampling the synthetic aperture is usually performed so as to increase the area coverage rate (1). However, this has a main consequence. Ambiguous images (3), appear in addition to true target images. The imaging method of broadband SAS is a sonar technique, which, while operating under such stringent conditions, enables a maximum of useful information about the sonar target to be collected for processing. A

1077–2014/95/010019 + 13

wider bandwidth results in increased resolution in range direction. The azimuthal resolution is still determined by the dimension of the physical antenna (1), but image aliases which otherwise would characterize any other undersampled system are smeared into the image background (1,4). Therefore, it is evident that broadband SAS is capable of producing high resolution images, if a sensible processing scheme is applied to the raw data.

SAS-imaging is a classical example of a case where information about an object is acquired by monitoring backscattered acoustic signals. The treatment of the problem of retrieving an object function from its image by applying a computer algorithm to measured data, requires adequate description of the physical processes leading to image formation. In many cases of acoustical reflectivity imaging (5,6), such a mathematical model is given by the Fredholm integral equation of the first kind (7):

$$g(x, y) = \iint_D h(x, y; x_0, y_0)s(x_0, y_0)dx_0dy_0 \qquad [1]$$

where D is a region in $\mathbf{IR}^2$. In Eqn [1], h is a general kernel representing a point spread function. If s is the object function, then g is called the observation or the image. The underwater imaging technique of broadband SAS has access to the integral equation given above (8,9). Therefore, among the important points concerning broadband SAS, we note that the processing of raw data need not be restricted to the conventional methods (3,10,11) only. Since our purpose lies in imaging, all details regarding the sonar system used are not discussed. We refer the interested reader to work by de Heering *et al.* (12). For consistency, the PSF determined from parameters of the same sonar system has been used in all simulation experiments performed in this work. This also allows comparisons with previous work (12).

In this paper, we propose a relaxed gradient algorithm for reconstructing an object from broadband SAS-data. The derivation is based on a steepest descent approach to restoration. Properties of the true restoration error are directly incorporated into the reconstruction process through adaptive relaxation. Thus, the error is purposefully suppressed, leading to improved rate of convergence at an early phase of the iteration process. The proposed algorithm, whose iterative nature offer several advantages over direct solution methods (13), is analysed and sufficient conditions for convergence are established. The form of the proposed algorithm is suitable for extending it to sharpen any matched filter-processed image.

The discussion of the mathematical model for the underlying physical problem is presented next. Later, we derive and analyse the relaxed gradient algorithm. Finally experimental results using simulated data are shown, along with limitations of the proposed algorithm.

Processing of Broadband SAS-data

Conventional processing methods apply a pulse compression technique (which is essentially a digital matched filter) to the SAS-data, followed by aperture synthesis (3), in order to improve resolutions in range and azimuthal directions respectively. But, to exploit the high resolution capabilities of SAS-systems fully, focused coherent processing is used for aperture synthesis (4,11). In this case, the two-step process is equivalent to a two-dimensional matched filtering between a received signal g and its replica, which is identified as the PSF h of the imaging system (9). Thus, we obtain the following expression

$$\begin{aligned} s_{mf}(x, y) &= \iint_D g(x + x_0, y + y_0)h(x_0, y_0)dx_0dy_0 \\ &= h(x, y) \otimes\otimes g(x, y) \end{aligned} \qquad [2]$$

where s_{mf} is the focused image, and $\otimes\otimes$ denotes two-dimensional correlation. The matched filter focusing technique in Eqn [2] can be shown to be equivalent to the following expression

$$s_{mf}(x, y) = s(x, y) ** R_{hh}(x, y) \qquad [3]$$

where R_{hh} is the autocorrelation of the PSF, and ** stands for two-dimensional convolution. From Eqn [3], we conclude that matched filter processing is suboptimal, because the estimate is equal to the original object reblurred with the autocorrelation of the PSF, and in practice, it is unlikely that the autocorrelation, R_{hh} will be an impulse. It is clear from Eqn [3], that the image details lost during conventional processing can be regained using an image deblurring algorithm for postprocessing.

Alternatively, a deconvolution method can be applied directly to focus the SAS-data. We note that if the imaging process is restricted to those objects within range and cross-range limits such that the PSF remains range-invariant, and is therefore independent of absolute position, the data

acquisition model given by Eqn [1] reduces to the simpler convolutional integral

$$g(x, y) = \iint_D h(x - x_0, y - y_0)s(x_0, y_0)dx_0dy_0$$
$$= s(x, y) ** h(x, y) \quad [4]$$

Thus, in the event that the inverse of the operator h exists, the object can be reconstructed by the deconvolution operation as

$$s = g(**)^{-1}h \quad [5]$$

However, direct deconvolution, which is equivalent to applying an inverse filter to the problem (14), will not deliver satisfactory results, since there is no guarantee that the integral kernel h is not ill-conditioned. Iterative deconvolution has been applied by de Heering *et al.* (12) to focus SAS-data. In a real system the iterative algorithm is expected to execute within a unit of time, which a conventional processing scheme would require to produce the image. Therefore, we propose the development of a fast reconstruction method utilizing iterative methods, that performs at near real-time, as compared to the matched filter, or its equivalence.

Optimal Iterative Algorithm for Reconstruction

The field of image restoration has received wide attention from the engineering and scientific community. The comprehensive paper by Biemond *et al.* (13) cites over 80 publications on the subject. Many algorithms have been published, ranging from the empirical formula of van Cittert (15) over ones with optimized rates of convergence (16) to computationally intensive methods incorporating regularization (17), adaptivity based on the human visual system (18), higher order convergence (19), etc. Much of the published work is directed at problems in the field of optical imaging, where deblurring is performed as a postprocessing operation and time may not be a deciding factor. In applications such as focussed processing of raw SAS-data, or computerized tomographic imaging with ultrasound sources, it is necessary to design reconstruction algorithms which are computationally efficient and show sufficient accuracy within a few iterations, thus enabling fast processing of the information delivered by the sensor. Furthermore, deblurring is secondary, the primary aim is in reconstruction. These aspects motivate us to search for a restoration method which is specifically optimal to the requirements dictated by the application. The algorithm to be presented is therefore derived from basic methods of optimization theory (20–22) and is made specific to solving the problem of SAS-data processing.

Problem Statement and Solution Method

The integral-equation in Eqn [1] is a two-dimensional inverse problem (23). For the discussion to follow, it is convenient to restate it using matrix-vector notation

$$\mathbf{g} = \mathbf{Hs} + \mathbf{n} \quad [6]$$

s, g, n are lexicographically ordered vectors of size $N^2 \times 1$(24,25) and **H** is the distortion operator of size $N^2 \times N^2$, whose elements are samples of the PSF. The additive term, **n**, represents the noise associated with the measurement process. In the general case, when discrete values are not considered, Eqn [6] still holds if it is written in operator notation as in Schafer *et al.* (26). In previous parts of this paper, the physics of SAS-image formation was modelled by a Fredholm integral equation of the first kind. The ill-posed nature of the solution (27) translates into an ill-conditioned matrix **H**. This problem, together with the difficulties encountered when **H** is singular (17), can be tackled implicitly, if the solution is sought utilizing an iterative procedure. Iterative gradient methods are extensively used to solve problems involving minimization of functionals. The behaviour of a gradient method for a general function is similar to its behaviour for a quadratic function. Therefore, it is instructive to consider first the case in which the function to be minimized is quadratic and relate the method to the underlying problem. It has been shown in optimization theory (20,22), that gradient methods which minimize the quadratic function

$$f(\mathbf{u}) = \frac{1}{2}\mathbf{u}^T\mathbf{Au} - \mathbf{v}^T\mathbf{u} + c_1 \quad [7]$$

solve a linear system similar to Eqn [6], that is

$$\mathbf{v} = \mathbf{Au} \quad [8]$$

A sufficient condition for f to have a minimum is that its Hessian **A** be positive definite. But here, we consider a more general case where the only condition on **A** is that it should

be a symmetric matrix. The optimal gradient algorithm (22) is an iterative technique which successively approximates the solution to Eqn [8] by performing the following computations:

$$\mathbf{u}_1 = \mathbf{v};$$

$$\mathbf{u}_{k+1} = \mathbf{u}_k + a_k \mathbf{r}_k \qquad [9a]$$

In Eqn [9a], if the correction vector, $\mathbf{r}_k$, is chosen to be the negative gradient of the quadratic function as

$$\mathbf{r}_k = -\nabla f(\mathbf{u}_k) \qquad [9b]$$

which happens to be the direction of steepest descent of f, then the algorithm is called the method of steepest descent (28), and the optimal step size a is determined such that

$$a = a_k \text{ minimizes } f_k(a) = f(\mathbf{u}_k + a_k \mathbf{r}_k) \qquad [9c]$$

Keeping in mind that the ultimate aim in Eqn [6] is to obtain a restored solution $\hat{\mathbf{s}} \equiv \mathbf{s}_k$ rather than an explicit inversion, the algorithm can be applied to the image restoration problem, if a quadratic function describing some quantity specific to the problem can be found. To this purpose, the residual at k-th iteration is determined from Eqn [6] as

$$\mathbf{e}_k = \mathbf{g} - \mathbf{H}\mathbf{s}_k \qquad [10]$$

Its squared norm is quadratic in $\mathbf{s}_k$ as can be seen from the following expression

$$\begin{aligned} ||\mathbf{e}_k||^2 &= (\mathbf{g} - \mathbf{H}\mathbf{s}_k)^T (\mathbf{g} - \mathbf{H}\mathbf{s}_k) \\ &= \mathbf{s}_k{}^T (\mathbf{H}^T\mathbf{H})\mathbf{s}_k - 2(\mathbf{H}^T\mathbf{g})^T \mathbf{s}_k + c'_2 \end{aligned}$$

Thus, a quadratic function that describes the imaging problem can be written as

$$\begin{aligned} \phi(\mathbf{s}_k) &= \frac{1}{2} ||\mathbf{e}_k||^2 \\ &= \frac{1}{2} \mathbf{s}_k{}^T (\mathbf{H}^T\mathbf{H})\mathbf{s}_k - (\mathbf{H}^T\mathbf{g})^T \mathbf{s}_k + c_2 \end{aligned} \qquad [11]$$

Based on this, quantities corresponding to those in Eqns [9a–c] can be stated as follows:

$$\mathbf{s}_1 = \mathbf{H}^T \mathbf{g}$$

$$\mathbf{s}_{k+1} = \mathbf{s}_k + \beta_k \mathbf{p}_k \qquad [12a]$$

$$\mathbf{p}_k = -\nabla\phi(\mathbf{s}_k) = \mathbf{H}^T \mathbf{e}_k \qquad [12b]$$

$$\beta_k = \frac{(\mathbf{e}_k, \mathbf{H}\mathbf{p}_k)}{(\mathbf{p}_k, \mathbf{H}^T\mathbf{H}\mathbf{p}_k)} = \frac{||\mathbf{p}_k||^2}{||\mathbf{H}\mathbf{p}_k||^2} \qquad [12c]$$

Comparing the function in Eqn [11] to that in Eqn [7], it can be deduced, that the algorithm outlined in Eqns [12a–c] solves the system of equations

$$\mathbf{H}^T\mathbf{H}\mathbf{s} = \mathbf{H}^T\mathbf{g} \qquad [13]$$

Postponing the discussion of any necessary conditions on the parameter of β_k to a later section, it can be concluded from this result that the algorithm in Eqns [12a–c] converges to the minimum norm least squares solution plus $\mathbf{s}_O$, where $\mathbf{s}_O$ is any vector in the null space of $\mathbf{H}^T\mathbf{H}$ (29–31). Thus, it can be interpreted as an iterative least squares method with a locally optimized rate of convergence. If instead, the step size is held constant at a value that guarantees convergence of the sequence $\{\mathbf{s}_k\}$, then the algorithm reduces to the reblurred van Cittert method (32). The solutions of Eqn [13] contain those of Eqn [8], which may not have solutions depending on the properties of **A**.

Modification to the Basic Iterative Algorithm

The main issue of improved rate of convergence, while keeping computation to a minimum calls for a re-examination of the iteration procedure as a whole. It is obvious that the correction vector leads us into the convex set of points containing the solution, but the step size does not optimally penalize the true error. This can easily be inferred from Eqn [12c], whose derivation was based on a quadratic function that minimizes the squared norm of the residual, which is recognized to be the observable error in the image space. The true restoration error, however, is defined in the object space as

$$\xi_k = \mathbf{s} - \mathbf{s}_k \qquad [14]$$

From Eqns [10], [14] and Parseval's identity we have

$$|| \mathbf{e} ||^2 = || \mathbf{H}\xi ||^2$$

$$= \Delta_x \Delta_y \int_{-\frac{1}{2}\Delta y}^{\frac{1}{2}\Delta y} \int_{-\frac{1}{2}\Delta x}^{\frac{1}{2}\Delta x} | H(f_x, f_y) |^2 \, | \tilde{\xi}(f_x, f_y) |^2 \, df_x \, df_y \qquad [15]$$

where Δ_x, Δ_y are spatial sampling intervals, f_x, f_y are spatial frequencies, and $\tilde{\xi}(f_x, f_y)$ is the Fourier transform of ξ. Since the PSI of a real system is dissipative, that is, it can pass or attenuate energy at given frequencies, the norm of the residual cannot exceed that of the true restoration error, i.e., $||\mathbf{e}_k||^2 \leq ||\xi_k||^2$. This can have adverse effects on the rate of convergence. Specifically, more iterations will be required to achieve a prescribed degree of sharpness in the reconstructed image. A constant step size can be used at the cost of higher iterations or increased computation, if a higher-order algorithm (19) is implemented.

A numerically effective method for improving performance of the basic algorithm could be offered by a generalized relaxation technique. This hypothesis is made as a consequence of investigations, which prove that in using a steepest descent method, it is necessary to incorporate an under-relaxation parameter into the iteration process (22). Comparable techniques have been incorporated into the Jacobi iteration procedure (34), a method whose structure is quite similar to the algorithm in Eqns [12a–c]. Young (33) showed that better results can be gained by using variable relaxation, and in one case of technical interest, fixed and adaptive relaxation methods have been demonstrated (30). In this work, we propose the use of an adaptive relaxation technique following methods outlined by Hestenes (22) and Jennings & Mckeown (34), while simultaneously reducing the number of matrix computations per iteration. The problem encountered in many cases where dynamic or non-stationary relaxation (35) is to be performed, is that of how to determine the best weighting factor in each iteration. Chebyshev polynomials have been used by Richardson (33), but this increases computation. The method followed here begins with a modification of Eqn [12c] of the basic algorithm. In determining the step size, we replace the quadratic function through the squared norm of the true error to arrive at the following equations.

$$\Phi(\mathbf{s}_k) = \frac{1}{2} ||\xi_k||^2 \qquad [16]$$

$$\alpha = \alpha_k \text{ minimizes } \Phi_k(\alpha) = \Phi(\mathbf{s}_k + \alpha_k \mathbf{p}_k) \qquad [17]$$

This modification leads to a relaxed gradient algorithm of the form

$$\mathbf{s}_1 = \mathbf{H}^T \mathbf{g}$$

$$\mathbf{S}_{k+n} = \mathbf{S}_k + \alpha_k \mathbf{p}_k \qquad [18a]$$

$$\mathbf{p}_k = -\Delta\Phi(\mathbf{S}_k) = \mathbf{H}^T \mathbf{e}_k \qquad [18b]$$

$$\alpha_k = \frac{(\xi_k, \mathbf{p}_k)}{(\mathbf{p}_k, \mathbf{p}_k)} = \frac{||\mathbf{e}_k||^2}{||\mathbf{H}^T \mathbf{e}_k||^2} \qquad [18c]$$

We point out that the iterative process remains a steepest descent algorithm, because the correction vector has not been altered. Also, it's worth noting from Eqn [15] that $||\mathbf{e}_k||^2 = 0$ does not imply $||\xi_K||^2 = 0$, when $\mathbf{H}$ vanishes in some frequency bands. This confirms the hypothesis that the proposed relaxation is a better indicator for convergence. The result in Eqn [18c] is in principle a generalization of the error energy minimization (16) to multidimensional problems.

Convergence

In the literature, convergence of iterative algorithms like that in Eqns [18a–c] but with α set to a constant, is established using the properties of contractive and non-expansive mappings (26). Based on these theorems, it has been deduced, that the sufficient condition for convergence to a unique fixed point is for the operator $\mathbf{I} - \alpha\mathbf{H}^T\mathbf{H}$ to be contractive. But, for some distortions, $\mathbf{I} - \alpha\mathbf{H}^T\mathbf{H}$ is non-expansive, because the matrix $\mathbf{H}^T\mathbf{H}$ is allowed to be non-negative. Under these more general conditions, convergence is to the solution stated previously. In both cases the parameter α must be constrained as follows (18):

$$0 < \alpha < \frac{2}{M} \qquad [19]$$

where M is the largest eigenvalue of the symmetric non-negative matrix $\mathbf{H}^T\mathbf{H}$. The scanned literature on restoration methods reveals no explicit derivation of the above relations for cases with variable step size. Therefore, in order to establish convergence for the relaxed gradient algorithm,

we must generalize the steps which lead to the operator $\mathbf{I} - \alpha \mathbf{H}^T\mathbf{H}$ to iteration matrices (34). By examining the iteration Eqn [18a], we recognize that, applying contractive and non-expansive theorems is equivalent to the following sufficient condition. For absolute convergence, the upper bound of the sequence $\{\mathbf{S}_k\}$ generated from iterates in Eqn [18a], must be less than unity. For the type of algorithm represented by Eqns [18a–c], the upper bound can be written as (22)

$$L_0 = \lim_{k \to \infty} \sup ||\mathbf{I} - \alpha_k \mathbf{H}^T\mathbf{H}|| \qquad [20]$$

provided the sequence $\{\alpha_k\}$ is bounded. We conclude that for convergence, the iteration matrix $\mathbf{I} - \alpha_k \mathbf{H}^T\mathbf{H}$ must be at least non-expansive for some finite $k = n$. It has been proved (22) that if α_k is given by a formula such as Eqn [18c], in which $\mathbf{e}_k$ is any non-null vector, then for $n \leq k < \infty$, α_k satisfies the constraints in Eqn [19], which is the necessary condition. This completes convergence proof for the relaxed algorithm.

Implemented Form of the Proposed Algorithm

The asymptotic rate of convergence for the relaxed gradient algorithm is easily deduced by considering the error propagation through one iteration step to the next. Since the iteration matrix is the operator $\mathbf{I} - \alpha_k \mathbf{H}^T\mathbf{H}$, we have $\xi_{k+1} = (\mathbf{I} - \alpha_k \mathbf{H}^T\mathbf{H})\xi_k$. This is a linear rate of convergence, similar to that for the method of steepest descent. It leads to the belief that the method converges slowly and could probably be inferior. However, the estimates approach the exact solution much faster, mainly due to the fact that the adaptive relaxation makes implicit use of the information about the true error while the iterative process evolves. Because the error is being suppressed more purposefully, a significant improvement in efficiency is obtained. Visual convergence is likely to be discernible within a few iterations. Experiments show an even better performance during the initial phase of the iterative process, if α is replaced as given in Eqn [18c], through its square root. Noting that under these changed circumstances the conditions for convergence discussed earlier cannot be guaranteed, the relaxed algorithm must incorporate additional information to overcome any unwanted side-effects. Prior knowledge of the form of the solution, is widely used (26) in the form of constraints, to permit the convergence of an iterative formula that might not otherwise converge. Specifically, in the sonar case, it is known on physical grounds, that the object has a bounded support. This is a hard constraint and can be expressed using an operator $\mathbf{C}$. Therefore, the iterations can be carried out with $\mathbf{s}_k$ replaced by $\mathbf{C}\mathbf{s}_k$. Thus the implemented relaxed gradient algorithm can be stated as follows:

$$\mathbf{s}_1 = \mathbf{H}^T \mathbf{g} \qquad [21a]$$

$$\mathbf{s}_{k+1} = \tilde{\mathbf{s}}_k + \tilde{\alpha}_k \mathbf{p}_k \qquad [21b]$$

$$\tilde{\mathbf{s}}_k = \mathbf{C}\mathbf{s}_k \qquad [21c]$$

$$\tilde{\mathbf{e}}_k = \mathbf{g} - \mathbf{H}\tilde{\mathbf{s}}_k \qquad [21c]$$

$$\tilde{\mathbf{p}}_k = \mathbf{H}^T\tilde{\mathbf{e}}_k \qquad [21d]$$

$$\tilde{\alpha}_k = \frac{||\tilde{\mathbf{e}}_k||}{||\mathbf{H}^T \tilde{\mathbf{e}}_k||} \qquad [21e]$$

If the algorithm is applied to the SAS-problem, then the matrix $\mathbf{H}$ is Toeplitz. The algorithm Eqns [21a–e] can be written using signal notation:

$$s_1 = h \otimes\otimes g$$

$$s_{k+1} = cs_k + \tilde{\alpha}_k h \otimes\otimes (g - h^{**}cs_k)$$

$$\tilde{\alpha}_k = \frac{|\tilde{e}_k|}{|h \otimes\otimes \tilde{e}_k|} \qquad [22]$$

Note that conjugate matrix transpose results in correlation between the respective two-dimensional functions. The constraint operator is multiplicative, because it is enforced in spatial domain. The signal norm given in the last part of Eqn [22] is defined for the discrete signals used in the experiments as

$$|e_k| = \sqrt{\frac{1}{IJ} \sum_{i=1}^{I} \sum_{j=1}^{J} e_k^2 (i, j)} \qquad [23]$$

From Eqn [22], it can be seen that the relaxed gradient algorithm executes two computations per iteration, as compared to three for the steepest descent algorithm.

Two points can be noted as concerns the algorithm in Eqns [21a–e]. If focusing of the sonar data is to be performed using interative techniques, then its equivalent in Eqn [22] can be directly applied to the measured data. If a matched filter estimate of the object is available as s_{mf}, and postprocessing is required to sharpen the image, then the algorithm can be applied to Eqn [3] in a form similar to the reblurred van Cittert's method:

Setting $\alpha = 1$, that is, taking the non-optimized version of Eqn [21], we get

$$\begin{aligned} s_{k+1} &= cs_k + (R_{hg} - R_{hh} ** cs_k) \\ &= cs_k + (S_{mf} - R_{hh} ** cs_k) \end{aligned} \qquad [24]$$

In Eqn [24], the correlations are constant quantities which can be computed and stored, before the iterations commence. The only computation performed per iteration is a convolution. Thus, it can be seen from the last discussions in this section that the relaxed gradient algorithm is suitable for solving the problem of SAS-data processing.

Simulation Results and Applicability

In this section, we present results of numerical experiments performed using simulated test objects, supposed to present significant difficulties in underwater imaging. The geometry of the PSF, which is sketched out in Figure 1(a), corresponds to definitions of the SAS-design example from (9). The dimensions of 6·4m × 64m are due to a real situation that would occur at sea. The PSF and the test objects were used to test the performance of a reconstruction algorithm (12), and they have been used here for consistency. All figures presented, are defined as 64 × 64 matrices. The distances in range and azimuthal directions (sonar track) respectively, as given on the figures, indicate the difference in sampling. The algorithms have been implemented using two-dimensional FFT. To enable calibrated comparisons, all of the two-dimensional functions must be normalized. Although it was assumed that target insonification is done using broadband pulses implying that pulse compression is unnecessary, we still have to perform a two-dimensional matched filter on the received signals, because the imaging geometry leads to a PSF with a curvature as shown. The experimental work has been carried out using simulated test objects because we wanted reproducible characteristics, which can be used as markers.

Examples

In this numerical example, we want to evaluate the performance of the relaxed gradient algorithm, by comparing results to those obtained using the steepest descent, and the Bremen2 Algorithm (12). The latter is a SAS-focusing technique, which implements iterative deconvolution, and uses a correlation coefficient to accelerate convergence. The criterion used here is visually good convergence within a few number of iterations. In Figure 1(c), the observation g represents the raw data, collected by the SAS-system, if it were to image the crown or crater shown in Figure 1(b). For this simulation, it was calculated by convolving the PSF h with the crown s. Figures 2(a–c) show results obtained after 10 iterations using the three algorithms. The estimate after 10 iterates of the steepest descent method Figure 2(a) is judged poor. It does not show sufficient convergence. Bremen2 performs relatively well, but, there is a clear indication of energy leakage to the left and to the right in the reconstruction in Figure 2(b). In Figure 2(c), the relaxed gradient algorithm displays good restoration. Apart from a small incursion, there are no erroneous negative values, as is produced by the other two methods. This can be clearly seen from the slice taken across the range direction, approximately at the place with maximum loss Figure 2(d). The estimates after 50 iterations are similar for the first two algorithms. The results for the relaxed gradient algorithm Figure 3(c) is comparable to the crown itself. This can also be seen in Figure 3(d), where the amplitude is over 80% of the original. These results confirm the ideas proposed earlier, and considered in the development of the relaxed gradient algorithm.

Target 19, which is shown in Figure 4(a), is an object designed to present a more realistic situation of SAS-imaging, e.g., an iceberg. Its size and form do not allow simple definition of a hard constraint on the 64 × 64 raster. Therefore, it presents significant reconstruction difficulties. The results obtained for 10, 24, and 100 iterations are shown in Figures 4(c–e), along with that for 100 iterations of Bremen2 Figure 4(f), and the matched filter estimate Figure 4(b). It is worth noting, that the new algorithm shows superconvergence at the 100-th iterate, although at 10 iterations, unwanted peaks appear due to a non-symmetrical constraint.

Significance for SAS-data processing and related Applications

Qualitative improvement in resolution is evident in the reconstructions performed with the relaxed gradient algo-

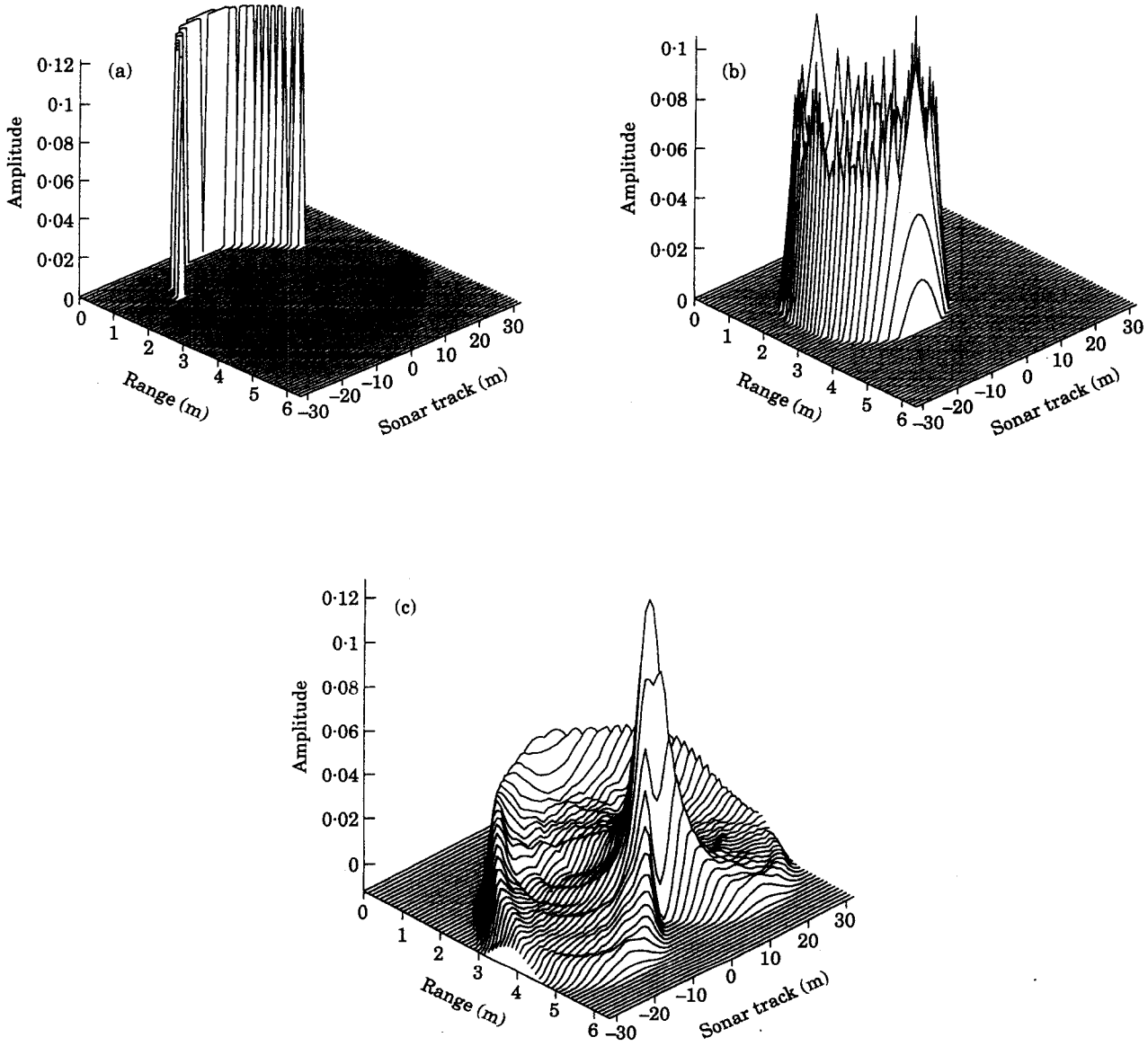

Figure 1. Test data used in the experiments. (a) The point spread function; (b) Crown; (c) Observation.

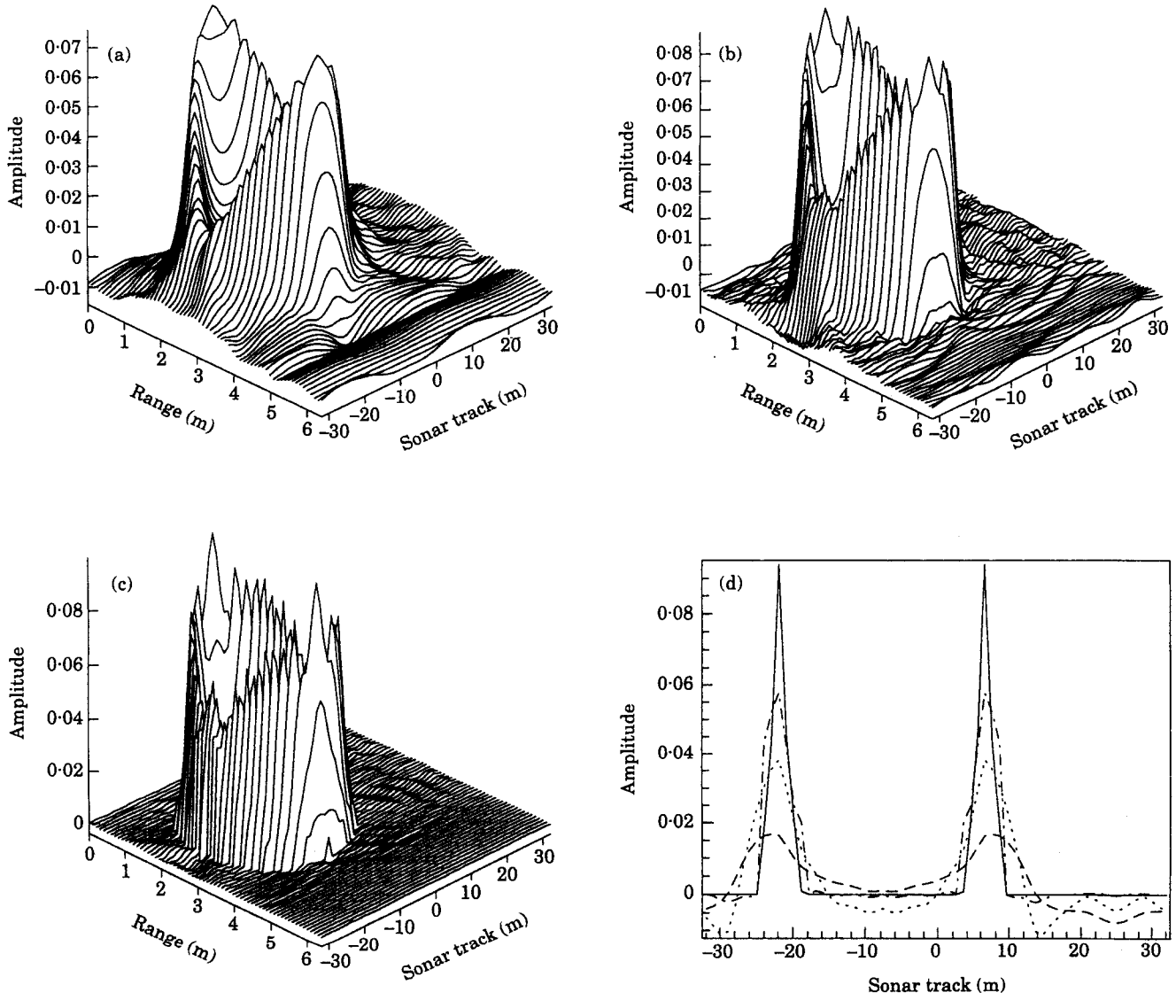

Figure 2. Restoration after 10 iterations. (a) Steepest descent algorithm; (b) Bremen2 algorithm; (c) Relaxed gradient algorithm; (d) Slice parallel to sonar track. —, original; — — —, steepest descent; ·····, Bremen2; –·–·–·, relaxed gradient.

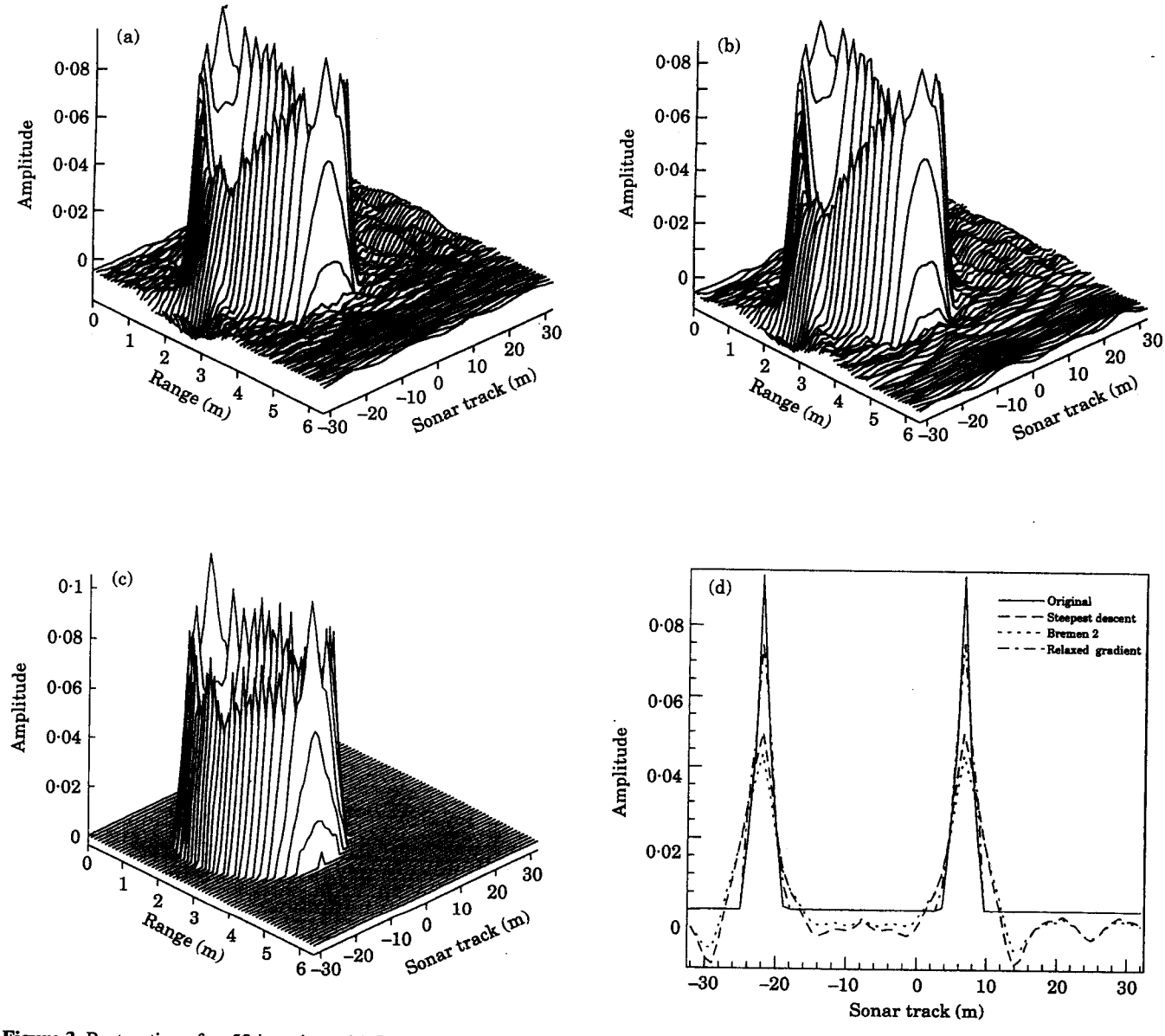

Figure 3. Restoration after 50 iterations. (a) Steepest descent algorithm; (b) Bremen2 algorithm; (c) Relaxed gradient algorithm; (d) Slice parallel to sonar track. —, original; — — —, steepest descent; ·····, Bremen2; -·-·-·, relaxed gradient.

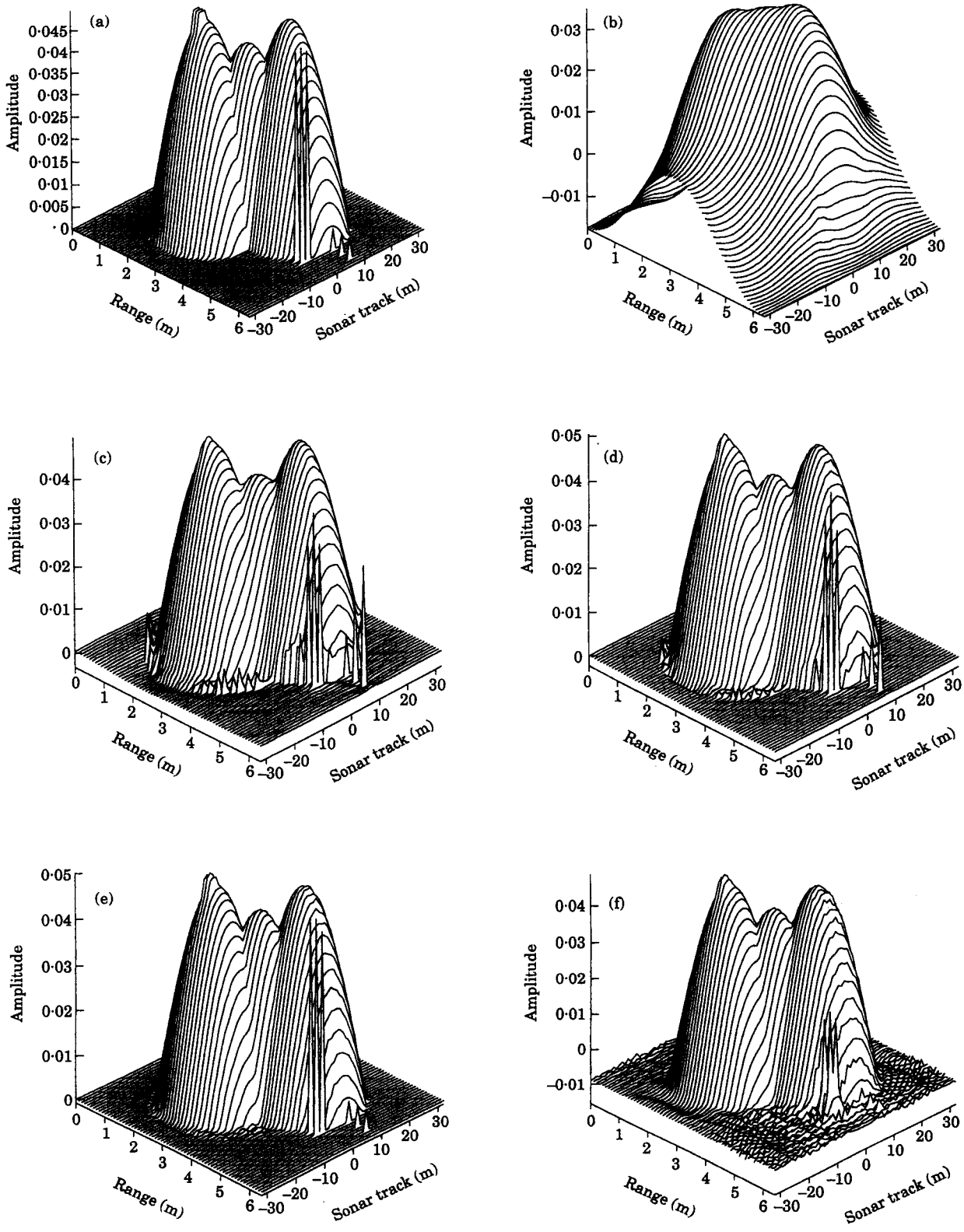

Figure 4. Application of relaxed gradient algorithm to target 19. (a) Target 19; (b) Matched filter reconstruction; (c) Reconstruction after 10 iterations; (d) Reconstruction after 24 iterations; (e) Reconstruction after 100 iterations; (f) Bremen2 algorithm after 100 iterations.

rithm. A main problem is constraint tightness, which leads to some errors at low iterations, but the sharp features in target 19 are visible. This confirms that more image detail is displayed than those achievable by matched filter processing. One important point to note is that an iterative reconstruction method as the one presented, demands that the point spread function of the imaging system be known. This is a problem, which in applications like optical image restoration, extends deblurring to include system identification (13) as well. In the sonar case, the PSF is either only approximately known, or has to be recovered from field data. This can be accomplished by insonifying a reflecting object, whose range and azimuthal dimension is small with respect to the range and azimuthal resolution of the sonar. In this case, the object in question is effectively a point target. If, on the other hand, an image produced by a conventional focusing technique requires postprocessing to bring out more image detail, then the same conventional processing scheme can be used to extract the autocorrelation of the point spread function necessary for deblurring according to the algorithm in Eqn [24].

Processing of data from range dependent point spread functions has been discussed by de Heering (9). In this paper, we considered the sonar to be operating in the Fresnel zone (1), where the asumption of range-invariance is well approximated.

In its operation, undersampled broadband SAS spreads azimuthal aliases into the image background. This is a form of self-clutter and may increase the background noise. If the phenomena can be modelled as additive noise as in Eqn [6], then the convergence conditions cannot be fulfilled, unless suitable regularizing operators are included. This could offset the objective followed here to achieve absolute low-cost computation. Difficulties are also encountered when the position of the constraint operator has to be determined. As has been observed in the simulation with target 19 test function, the algorithm is sensitive to position of the constraint with respect to the true position of the object to be reconstructed. If, in this case, a usable constraint function cannot be obtained through clipping the first estimate, which is essentially the matched filter processed image, then it is advisable to use the unconstrained iteration, but the relaxation must be performed using the full value of α given in Eqn [18c].

Conclusions

This paper has discussed the development of an iterative restoration algorithm and its application to the problem of SAS-data processing has been demonstrated by examples. The development was based on an optimization theory approach to minimization of quadratic functions. Restrictions due to requirements of the application were used as guidelines to arrive at a simple, but robust algorithm, which show good convergence after a minimal number of iterations. The iterative structure of the algorithm offer an advantage over direct inversion, because deterministic knowledge about the original object can be incorporated into the reconstruction process, and thus improve convergence. It is concluded from this work, image restoration has reached maturity, but specific problems demand specific solutions, which is true for SAS-data processing.

Acknowledgements

We are indebted to Dr. K.U. Simmer, Bremen, Germany for providing us with private graphics-software used to draw the figures. The first author (E.O.) wishes to acknowledge the support of Dr. K.U. Simmer in the course of this work. We also thank the reviewer whose comments helped us sharpen our presentation and improve the overall clarity of this paper.

References

1. de Heering Ph. (1984) Alternate schemes in synthetic aperture sonar processing. *IEEE J. Ocean. Eng.*, **9**: 277–280.
2. Gough, P.T. (1986) A synthetic aperture sonar system capable of operating at high speed in turbulent media. *IEEE J. Ocean. Eng.*, **11**: 333–339.
3. Cutrona, L.J. (1975) Comparison of sonar system performance achievable using synthetic aperture techniques with the performance achievable by more conventional means. *J. Acoust. Soc. Am.*, **58**: 336–348.
4. Hayes, M.P. & Cough, P.T. (1992) Broad-band synthetic aperture sonar. *IEEE J. Ocean. Eng.*, **17**: 80–94.
5. Duchêne, B., Lesselier, D. & Tabbara, W. (1985) Diffusion tomography approach to acoustical imaging and media characterization. *J. Opt. Soc. Am. A*, **2**: 1943–1952.
6. Kak, A.C. & Slaney, M. (1988) *Principles of Computerized tomographic imaging*, New York, IEEE Press.
7. Hassani S. (1991) *Foundations of Mathematical Physics*, Boston, Allyn and Bacon.
8. Vant, M.R. (1983) SAR digital signal processing at CRC. In: Proceedures. IEEC, 122–125.
9. de Heering, Ph. (1990) Acoustic synthetic aperture processing – theory and applications, Ph.D. dissertation, University of Bremen, Bremen, Germany.
10. Rihaczek, A.W. (1969) *Principles of High Resolution Radar*, New York, McGraw-Hill.
11. Chatillon, J., Bouhier, M.-E. & Zakharia, M.E. (1992) Synthetic aperture sonar for seabed imaging: Relative merits of narrow-band and wide-band approaches. *IEEE J. Ocean. Eng.*, **17**: 95–105.
12. de Heering, Ph., Simmer, K.-U., Ochieng-Ogolla, E. & Wasiljeff, A. (1994) A deconvolution algorithm for broadband synthetic aperture data processing. *IEEE J. Ocean. Eng.*, **19**: 73–82.
13. Biemond, J., Lagendijk, R.L. & Mersereau, R.M. (1990) Iterative methods for image deblurring. *Proc. IEEE*, **78**: 856–883.
14. Andrews, H.C. & Hunt, B.R. (1977) *Digital Image Restoration*, Englewood Cliffs, NJ, Prentice-Hall.

15. Frieden, B.R. (1975) Image enhancement and restoration, In: Huang, T.S., ed., *Picture Processing and Digital Filtering*. New York, Springer-Verlag.
16. Prost, R. & Goutte, R. (1984) Discrete constrained iterative deconvolution algorithms with optimized rate of convergence. *Signal Processg*, **7**: 209–230.
17. Katsaggelos A.K. (1989) Iterative image restoration algorithms. *Optical Engg*, **28**: 735–748.
18. Katsaggelos, A.K., Biemond, J., Schafer, R.W. & Mersereau, R.M. (1991) A regularized iterative image restoration algorithm. *IEEE Trans, Signal Proc.*, **39**: 914–929.
19. Morris, C.E., Richards, M.A. & Hayes, M.H. (1988) Fast reconstruction of linearly distorted signals. *IEEE Trans. Acoustics, Speech and Signal Proc.*, **36**: 1017–1025.
20. Aoki, M. (1972) *Introduction to Optimization Techniques*. New York, Macmillan.
21. Fletcher, R. (1980) *Practical Methods of Optimization. Volume 1: Unconstrained Optimization*. Chichester, John Wiley and Sons.
22. Hestenes, M. (1980) *Conjugate Direction Methods in Optimization*. New York, Springer-Verlag.
23. Baltes, H.P., ed. (1978) *Inverse Source Problems*. New York, Springer-Verlag.
24. Pratt, W.K. (1975) Vector space formulation of two-dimensional signal processing operations. *Computer Graphics Image Processg*, **4**: 1–24.
25. Jain, A.K. (1989) *Fundamentals of Digital Image Processing*. Englewood Cliffs, NJ, Prentice-Hall.
26. Schafer, R.W., Mersereau, R.M. & Richards, M.A. (1981) Constrained iterative restoration algorithms. *Proc. IEEE*, **69**: 432–450.
27. Zuhair Nashed, M. (1981) Operator-theoretic and computational approaches to ill-posed problems with applications to antenna theory. *IEEE Trans. Antennas and Prop*, **29**: 220–231.
28. Ichioka, Y., Takubo, Y., Matsuoka, K. & Suzuki, T. (1981) Iterative image restoration by a method of steepest descent. *J. Optics (Paris)*, **12**: 35–41.
29. Bialy, B. (1959) Iterative Behandlung linearer Funktionalgleichungen. *Arch. Ration. Mech. Anal.* **4**: 166–176.
30. Tom, V.T., Quatieri, T.F., Hayes, M.H. & McClellan, J.H. (1981) Convergence of iterative nonexpansive signal reconstruction algorithms. *IEEE Trans. Acoustics, Speech and Signal Proc.*, **29**: 1052–1058.
31. Trussell, H.J. (1983) Convergence criteria for iterative restoration methods. *IEEE Trans. Acoustics, Speech and Signal Proc.*, **31**: 129–136.
32. You, Y.-Li. & Kaveh, M. (1993) Regularization and image restoration using differential equations. In: *Proc. IEEE Intt. Conf. Acoustics Speech and Signal Proc.*, **5**: 285–288.
33. Young, D. (1971) *Iterative Solution of Large Linear Systems*. New York, Academic Press.
34. Jennings, A. & McKeown, J.J. (1992) *Matrix Computation*. 2nd edn. Chichester, John Wiley & Sons.
35. Marchuk, G.I. (1975) *Methods of Numerical Mathematics*. New York, Springer-Verlag.